Transport of Pure Components in Pervaporation through a Microporous Silica Membrane

Ben Bettens,* Sofie Dekeyzer, Bart Van der Bruggen, Jan Degrève, and Carlo Vandecasteele

Department of Chemical Engineering, K.U. Leuven, W. de Croylaan 46, B-3001 Leuven, Belgium

Received: December 2, 2004; In Final Form: January 20, 2005

The pervaporation mechanism of pure components through a commercial microporous silica membrane was studied by performing experiments using water, methanol, ethanol, 2-propanol, and *n*-propanol in the 40−80 °C temperature range. Experimental fluxes were correlated to feed temperature and viscosity. It was found that the permeation mechanism obeys the adsorption−diffusion description, covering both the microscopic models based on configurational (micropore) diffusion and on activated surface diffusion. The contribution of convection was negligible. Size parameters for the permeating molecules such as molecular weight, kinetic diameter, and effective diameter, which are expected to have an influence on diffusion, did not correlate with the flux, thus strongly emphasizing the importance of sorption as the rate-determining step for transport in the pervaporation process. This was confirmed by correlating parameters reflecting polarity with flux: an exponential relation between the Hansen polarity (especially the hydrogen bonding component) and the flux was observed. A similar correlation was found between the dielectric constant and the flux. Furthermore, the flux increases in the same direction as the hydrophilicity of the pure components (log *P*). The effects of membrane surface tension and contact angles are less outspoken, but experiments performed on glass supported and silica supported membrane top layers suggest an important influence of the sublayers on the flux.

1. Introduction

Inorganic pervaporation membranes are more resistant to harsh chemical, thermal, and pressure conditions than polymeric membranes, enabling operation at elevated temperatures in a wide pH range in organic solvents, beyond the limitation of dissolving, swelling, and compacting the membrane.[1−5] The disadvantages of inorganic membranes are their brittleness and the higher production costs.[1,6,7]

Inorganic membranes consist of a (usually ceramic) supporting system and the final (usually ceramic) separation layer. The supporting system can be a single plate, tube, hollow-fiber, or honeycomb structure. The final separation layer can be porous or dense and single phase or composite. A system of macro-, meso-, and microporous layers can be built to meet specific applications.[6,8] Present research focuses on finding the optimal membrane material(s) in terms of separation factor, flux, and stability.[9] In this perspective, pervaporation membranes with an active layer of zeolite or amorphous silica on porous supports of alumina or stainless steel have become commercially available.[1,4,6]

To aid in further development of high-flux, tailor-made membranes, good insight into membrane performance (flux, selectivity) and into controlling processes (microstructural features, process conditions, solvent parameters) is essential. In the literature, many models are put forward to describe the transport through inorganic membranes.[10−14]

Also, different mechanisms were proposed, accounting for the selectivity of the active layer of inorganic membranes: in some cases, adsorption and diffusion play a major role; in other cases, molecular-sieve effects dominate.[6,15−22] Nevertheless, the exact transport/separation mechanism is not yet fully understood.

In this study, the performance of a commercial microporous silica membrane is characterized in terms of the pervaporation flux for five pure components (water, methanol, ethanol, 2-propanol, and *n*-propanol).

The first objective of the study is to gain more insight into the microstructural architecture of the hollow silica fiber. The experimental flux is correlated to feed temperature and viscosity to elucidate the mechanism of pure component transport, which depends on the pore size (section 2).

The second objective is to determine which pure component and membrane parameters play a role in the observed transport mechanism. Here, flux is correlated to the molecular weight, kinetic diameter, Hansen solubility, dipole moment, surface tension, dielectric constant, and contact angle of the liquid.

2. Theory

Inorganic microporous membranes have permanent pore structures with a given pore size distribution. Depending on the pore size, different mechanisms dominate the mass transport of pure components through a silica membrane. Table 1 gives an overview of the most important flow mechanisms as a function of pore diameter.

In the convective or viscous flow regime, mass is transported through large pores (>20 nm) by the bulk motion of the fluid. The molar flux through the inorganic membrane is described either by the Hagen−Poiseuille or the Kozeny−Carman relation, depending on the tortuosity of the pores.[1,6]

In addition to transport by the bulk motion of the fluid, mass may also be transported by molecular motion (diffusion). In pervaporation, it is thereby often assumed that the pure components are transported as gaseous species.[6]

(1) At large pore diameters (d_p > 10 nm), the process is that of bulk, concentration, or ordinary diffusion. Fick's law is used to describe binary or self-diffusion in gases. For multicomponent diffusion in gases, the Stefan−Maxwell expressions are used.[15,16]

* Corresponding author. Phone: +32 16 32 23 44. Fax: +32 16 32 29 91. E-mail: ben.bettens@cit.kuleuven.ac.be.

10.1021/jp044515e CCC: $30.25
Published on Web 02/25/2005

TABLE 1: Transport Regimes for Pure Components in Inorganic Membranes

flow mechanism	pore diameter	ref
convective flow (viscous, laminar, or Poiseuille)	>20 nm	1, 6
molecular diffusion	10 nm	15, 16
Knudsen diffusion (gas translation)	2−100 nm	6, 15−22
molecular sieving (configurational (micropore) diffusion)	<1.5 nm	6, 17−22
surface diffusion		6, 17−22
activated Knudsen diffusion (activated gas translation)		17, 18
capillary condensation		6, 20

(2) With decreasing pore diameter, the number of molecule-to-wall collisions becomes strongly dominant over the number of molecule-to-molecule collisions. The flow of a single gas in a long capillary can then be described by the Knudsen equation.[6,15−22]

(3) For the smallest pores (<1.5 nm), configurational (micropore) diffusion dominates.[6,17−22] Since flux increases exponentially with temperature, configurational diffusion is an activated process. The transition from Knudsen to configurational diffusion occurs when the size of the molecules approaches the pore diameter. Hence, the shape (configuration) of the molecules determines diffusion.

(4) For somewhat larger pores, surface diffusion (also activated) dominates.[6,17−22] It is a rather complex phenomenon that occurs when the pore walls strongly adsorb gas molecules. Three main groups of mechanisms of (monolayer) surface diffusion can be distinguished, varying from hydrodynamic flow in which the adsorbed gas is considered as a liquid film sliding along the surface under the influence of a pressure gradient to Fickian and hopping models. The latter assume that the molecules can move from site to site over a given distance across the surface and with a given velocity, passing energy barriers of a given height in the surface (activated diffusion jumps).[6]

(5) In the region between Knudsen diffusion and configurational diffusion, the molecules inside the micropores retain a gaseous character, although their movement becomes restricted and has to overcome certain energy barriers imposed by the micropore channels. Transport occurs in the activated Knudsen regime (activated gas translation).[17,18]

(6) Finally, at high pressures, capillary condensation leads to liquid filling the smaller pores, thus blocking the transport of vapor through those pores. Capillary condensation of pure liquids is described by the Kelvin equation.[6,20]

In this paper, two different approaches to describe the permeation process are experimentally tested.

The first is the pore flow model in which pervaporation is described as liquid permeation followed by vapor permeation through small pores, due to a pressure difference over the membrane. Convective transport is assumed within the pores with a phase change occurring when the pressure inside the membrane falls below the vapor pressure.[10,11] The molar flux is defined by eq 1 (Hagen−Poiseuille) or eq 2 (Kozeny−Carman):[1]

$$J_{vis} = \frac{\epsilon}{\tau}\frac{r_p^2}{8\eta}\frac{P_m}{RT}\frac{\Delta P}{L} \quad (1)$$

$$J_{vis} = \frac{\epsilon^3}{K\eta S^2(1-\epsilon)^2}\frac{P_m}{RT}\frac{\Delta P}{L} \quad (2)$$

where ϵ is the porosity, τ the tortuosity, η the viscosity of the pure component, K the Kozeny−Carman constant, S the internal surface area, r_p the pore radius, P_m the mean pressure over the membrane, R the gas constant, and L the membrane thickness. Assuming ideal gas behavior, the concentration of gas molecules in the membrane is approximated by $c = P_m/RT$.[17]

The second is the adsorption−diffusion model for ceramic membranes, analogous to the solution−diffusion model for polymeric membranes. It considers the membrane to be dense, so that only diffusion and no convection can occur. The transport consists of three consecutive steps: sorption onto the membrane, diffusion through the membrane, and desorption at the permeate side of the membrane (usually not explicitly considered, since mostly very fast).[10,11] The phenomenological adsorption−diffusion description is used to cover both the microscopic models based on configurational (micropore) diffusion and on surface diffusion. The molar fluxes for both activated mechanisms are defined by eqs 3 (surface diffusion) and 4 (molecular sieving), assuming Henry's law applies.[23] This means that at low levels of adsorption the concentration of a component in the membrane is proportional to the vapor pressure in the membrane pores, $c = SP$, where S is the adsorption coefficient or the solubility, a measure of the amount of penetrant sorbed by the membrane under equilibrium conditions.

$$J_{surf\text{-}diff} = SD_{surf\text{-}diff}\frac{\Delta P}{L} = S_0 \exp\left(\frac{\Delta H_S}{RT}\right) D_0 \exp\left(-\frac{E_D^{surf\text{-}diff}}{RT}\right)\frac{\Delta P}{L} \quad (3)$$

$$J_{mol\text{-}siev} = SD_{mol\text{-}siev}\frac{\Delta P}{L} = S_0 \exp\left(\frac{\Delta H_S}{RT}\right) D_0 \exp\left(-\frac{E_D^{mol\text{-}siev}}{RT}\right)\frac{\Delta P}{L} \quad (4)$$

S_0 and D_0 are pre-exponential factors, ΔH_S is the heat of adsorption, and $E_D^{surf\text{-}diff}$ and $E_D^{mol\text{-}siev}$ are activation energies of diffusion. In the adsorption−diffusion description, eqs 3 and 4 are both represented by eq 5.[19]

$$J_{ads\text{-}diff} = SD_{ads\text{-}diff}\frac{\Delta P}{L} = S_0 \exp\left(\frac{\Delta H_S}{RT}\right) D_0 \exp\left(-\frac{E_D}{RT}\right)\frac{\Delta P}{L} \quad (5)$$

E_D is the activation energy of diffusion according to the adsorption−diffusion model.

The transmembrane partial pressure difference, ΔP (identical to the feed vapor pressure for pure components, since $P_{perm} \ll P_{feed}$), is a function of temperature via the Clausius−Clapeyron equation (eq 6)

$$P^{vap} = A \exp\left(-\frac{\Delta H^{vap}}{RT}\right) \quad (6)$$

where A is a constant and ΔH^{vap} the heat of vaporization.

The overall temperature dependency of the flux follows an Arrhenius (exponential) type of relation (eq 7)[24]

$$J = J_0 \exp\left(-\frac{E_J}{RT}\right) \quad (7)$$

where $E_J = E_D - \Delta H_S + \Delta H^{vap}$ is the activation energy of the flux relation.

It is often more useful to describe the transport in terms of the membrane thickness normalized permeability coefficient, F (eq 8),[23]

$$F = \frac{J}{\Delta P} = \frac{SD}{L} = \frac{S_0 D_0}{L} \exp\left(\frac{\Delta H_S - E_D}{RT}\right) \qquad (8)$$

so that the activation energy of permeability is $E_F = E_D - \Delta H_S$. The difference in activation energy of flux and permeability is caused by the temperature dependency of the driving force ΔP.

In surface diffusion, the energy difference, E_F, can be positive or negative, depending on whether the transport activation energy exceeds the heat of adsorption or not. When $E_F < 0$, transport will decrease with increasing temperature, and when $E_F > 0$, it will increase with increasing temperature. Transport through molecular sieving always increases with temperature ($E_F > 0$).

3. Experimental Section

A tubular microporous silica membrane, supplied by Pervatech (Enter, The Netherlands) was studied. The ceramic tube had an inner diameter of 7 mm and an outer diameter of 10 mm and consisted of an α-alumina support, a γ-alumina intermediate layer, and a silica top layer coated on the inner surface of the hollow fiber. The effective membrane length and the effective membrane area were 23 cm and 50.58 cm^2, respectively. The mean pore size and the thickness of the silica layer were 0.3−0.55 and 10−20 nm, respectively.[25]

All pervaporation experiments were carried out with a laboratory test cell (lab test cell unit, Sulzer Chemtech, Neunkirchen, Germany). The initial setup contained a module for circular flat polymeric membranes but was modified as described in Van Baelen et al.[26] to incorporate a module for tubular ceramic membranes. Permeate was collected in glass traps cooled in liquid nitrogen in a Dewar flask. Vacuum was maintained using a two-stage vacuum pump. Permeate was collected by switching between two glass traps in parallel, so that the connection between the permeate side and the vacuum pump was never closed. Using this procedure, the permeate pressure was always below 10 mbar.

Experiments were performed with pure methanol, ethanol, 2-propanol, and *n*-propanol. According to recommendations from the producers, the membrane was not used with pure water, due to possible stability problems. Instead, mixtures of 90% water with 10% methanol or 10% ethanol were tested. Experiments were carried out in the 40−80 °C temperature range.

The pure components were all technical grade and were obtained from Merck (Amsterdam, The Netherlands). Data for molecular weight,[27−29] kinetic diameter,[30] viscosity,[27−29] Hansen parameter,[31−33] dipole moment,[34] log P,[35] and dielectric constant[34,36] were found in the literature. Effective diameters were calculated from the molecular structure and shape of the pure component with Hyperchem (release 2, 1991) as described by Van der Bruggen et al.[37] Contact angle measurements were performed on six flat, circular silica coated glass (three) and ceramic (three) plates that were heated for 5 h at 100 °C. A sessile drop approach was chosen, and a VCA Optima video camera system (AST Products, Billerica, MA) was used to measure the contact angles.[38]

For the mixtures of 90% water with 10% methanol or 10% ethanol, the permeate composition was calculated from the refractive index at 22 °C, which was determined by a refractometer. The partial feed pressure of the permeating component was calculated, using $P_{i,\text{feed}} = P_i^{\text{vap}} \gamma_i x_i$, where x_i is the molar fraction of component i in the liquid phase, γ_i the activity coefficient at temperature T (K), and P_i^{vap} the vapor pressure of pure i at temperature T (K). The values of γ_i were calculated with the UNIQUAC equation, and the values of P_i^{vap}, with the Clausius−Clapeyron equation. The partial permeate pressure was calculated using $P_{i,\text{perm}} = y_i P_{\text{perm}}$, where y_i is the permeate molar fraction and P_{perm} the total pressure.[39]

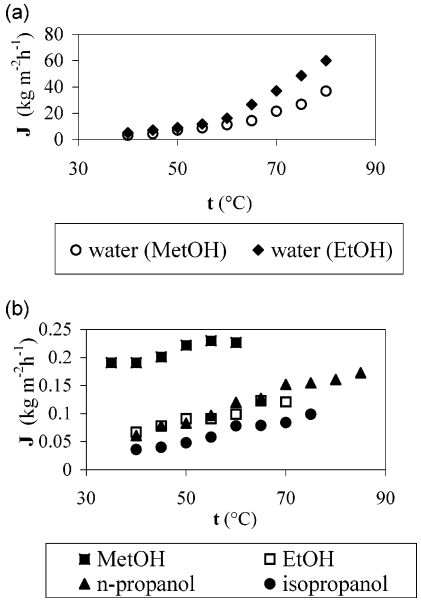

Figure 1. Mass flux, J, of (a) water and (b) alcohols as a function of temperature, t. According to recommendations from the producers, the membrane was not used with pure water, due to possible stability problems. Instead, mixtures of 90% water with 10% methanol or 10% ethanol were tested.

4. Results and Discussion

4.1. Pervaporation Results. Figure 1 shows the permeate mass flux as a function of temperature. The water fluxes (Figure 1a) are substantially higher (by a factor of 100) than the alcohol fluxes (Figure 1b). The flux of methanol is higher than that of the other alcohols. In addition, the temperature dependency suggests that the pervaporative transport is an activated process. The transport of water is more activated than that of the alcohols: the water flux increases more rapidly with temperature than the fluxes of the alcohols.

In Figure 2, the straight-line correlation between the logarithm of permeability, ln F, versus the inverse temperature suggests the applicability of the adsorption−diffusion model to describe transport through a silica membrane (eq 8). The activation energy of permeability, E_F, is found as the slope of the plotted line. The activation energy of permeability, E_F, of water is positive. In the case of the alcohols, E_F is negative, implying that the heats of adsorption, ΔH_S, are larger than the respective activation energies of diffusion, E_D (eq 8). Quantitative data for the activation energies of flux, permeability, and diffusion and for the heats of adsorption on silica as extracted from the experimental results in Figure 2 are listed in Table 2.

The activation energies of water flux (∼50 kJ/mol) are in the range 4−92 kJ/mol, as described by Feng et al.[24] for numerous membranes and binary aqueous systems. They are also comparable to those found by ten Elshof et al.[23] for similar aqueous mixtures. The activation energies of alcohol flux are significantly lower than those for water (7.4 kJ/mol for methanol

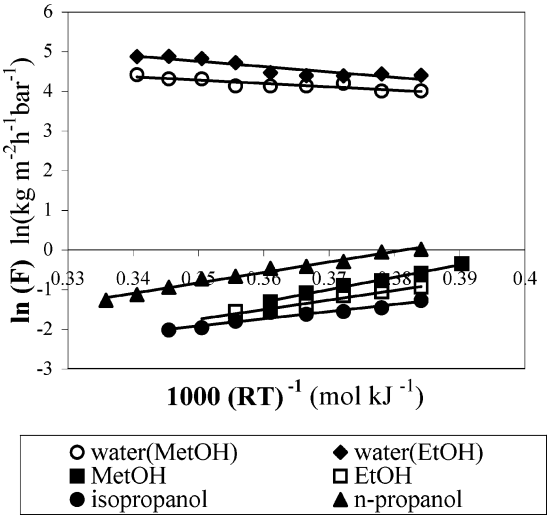

Figure 2. Logarithm of permeability, ln F, versus inverse temperature, T^{-1}. R is the universal gas constant. The continuous lines are linear fitted trend lines.

TABLE 2: Activation Energies of Flux, Permeability, and Diffusion in the Pervaporation of Pure Components and Heats of Adsorption on Silica[a]

	E_J (eq 9) (kJ/mol)	E_F (Figure 2) (kJ/mol)	ΔH_S[30] (kJ/mol)	$E_D = E_F + \Delta H_S$ (eq 11) (kJ/mol)
MetOH	7.4	−31.2	60−65	30−35
EtOH	17.7	−24.1	70	45
2-propanol	27.2	−18.1	N/A	N/A
n-propanol	21.6	−26.4	90	65
water (MetOH)	53.9	8.5	30−44	38−53
water (EtOH)	58.9	13.5	30−44	43−58

[a] N/A: not available.

and ~20 kJ/mol for the other alcohols). For methanol, the flux hardly changes with temperature.

The activation energies of permeability differ from the E_J values by the heat of vaporization, ΔH^{vap} (eq 7). All alcohols have a negative E_F value as a result of the large heats of adsorption. For molecules within the same functional group, adsorption strength increases as the number of carbon atoms increases.[30,40] On the other hand, the activation energy of diffusion also increases for larger molecules (and more rapidly) because of enhanced interactions with the pore wall. In general, the activation energy for nonpolar molecules increases with increasing kinetic diameter.[3,23] The positive activation energy of water is a result of substantial interactions with the pore wall upon diffusion (high E_D) because of the high polarity.

To verify if, besides diffusion, convective transport occurs (the basic assumption of the pore flow model), the permeability is plotted versus the inverse viscosity (Figure 3). In the case of convective transport, these should be linearly related, irrespective of the permeation temperature and the types of molecules (eq 1 or 2). This is not observed. Thus, the pore flow model is not appropriate to describe transport through a microporous silica membrane.

4.2. Influence of Solvent/Membrane Parameters on Flux. *Size Parameters.* According to the Stokes−Einstein equation,[37] molecular size has an influence on diffusion. The molecular size of a molecule can be characterized in many different ways: by the molecular weight, the Stokes diameter, the molar volume, the equivalent molar diameter, the effective molar diameter, the hydrodynamic volume, the number of methyl groups, the kinetic diameter, the Lennard-Jones length, or the van der Waals diameter.[37] Since it is not yet clear which size

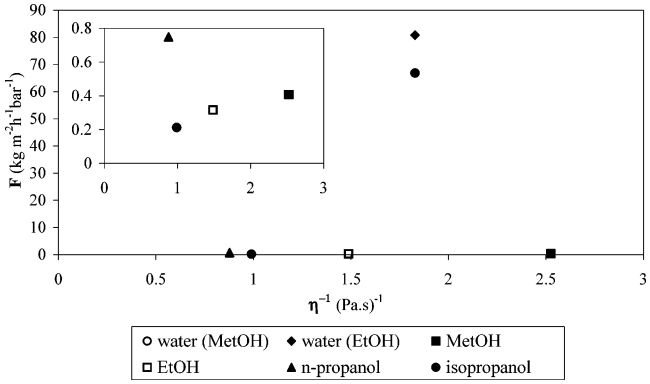

Figure 3. Permeability, F, as a function of inverse viscosity, η^{-1}, at 50 °C. The inset shows only the blown-up figure for the alcohols.

TABLE 3: Size Parameters

	molecular weight[27−29]	kinetic diameter[30] (nm)	effective diameter[37] (nm)
water	18.02	0.30	0.323
MetOH	32.04	0.38	0.566
EtOH	46.07	0.43	0.733
2-propanol	60.09	0.47	0.839
n-propanol	60.09	0.47	0.848

TABLE 4: Polarity Parameters

	dipole moment[34] (D)	dielectric constant[34,36]	Hansen parameter[31−33] (MPa$^{1/2}$) total	polar	disperse	hydrogen bonding
water	1.85	80	47.8	16.0	15.6	42.3
MetOH	1.70	33	29.6	12.3	15.1	22.3
EtOH	1.69	24.3	26.5	8.8	15.8	19.4
2-propanol	1.58	18.3	23.5	6.1	15.8	16.4
n-propanol	1.68	20.1	24.5	6.8	16.0	17.4

parameter is most suitable for explaining transport through micropores, Table 3 lists three often used parameters.

Table 3 and Figure 1 show that, in the low-temperature range (≤50 °C), the flux increases with decreasing molecular weight and decreasing kinetic diameter. Above 50 °C, however, the flux of *n*-propanol is slightly higher than the flux of the lower molecular weight component ethanol. The same conclusion holds for the effective diameter. Moreover, 2-propanol, which has a smaller effective diameter than *n*-propanol, has a smaller flux. Hence, there is no definite correlation between molecular size and flux, which means sorption effects are dominant over diffusion effects and are thus rate determining for the mass transport.

Polarity/Solubility Parameters. Polarity can be expressed by the dipole moment, the dielectric constant, or the Hansen parameter. The latter is the sum of a hydrogen bonding, a polar, and a disperse parameter.[33] The values for the different components are taken from the literature[31,32] and are given in Table 4.

In Figure 4, the flux at 50 °C is plotted against the total Hansen parameter. An exponential relation ($r^2 = 0.9940$) between the Hansen parameter and the flux is found (semilogarithmic graph). Especially the hydrogen bonding parameter shows a good exponential relation with the flux ($r^2 = 0.9792$, not shown). The polar parameter shows a fair correlation, but more scattered than the hydrogen bonding parameter ($r^2 = 0.8515$, not shown), while the disperse parameter has no correlation with the fluxes ($r^2 = 0.1283$, not shown). This indicates that sorption on the silica layer is mainly due to hydrogen bond formation. Similarly, an exponential relation ($r^2 = 0.9931$) was observed between the dielectric constant of the

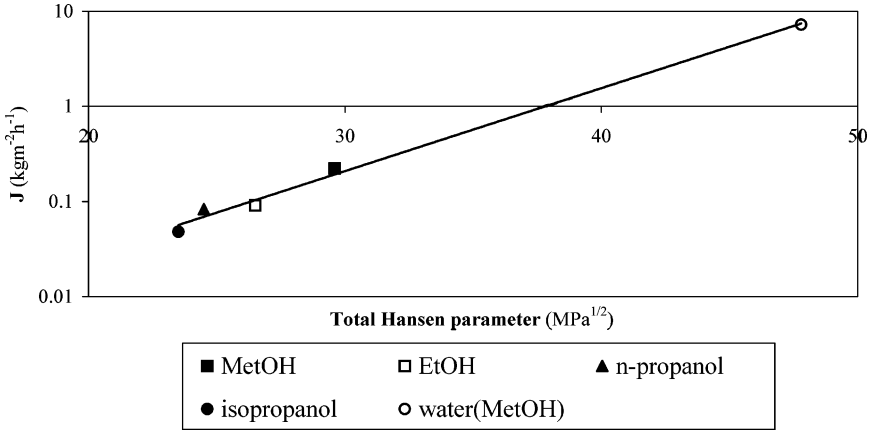

Figure 4. Flux, *J*, as a function of total Hansen parameter (all values taken at 50 °C).

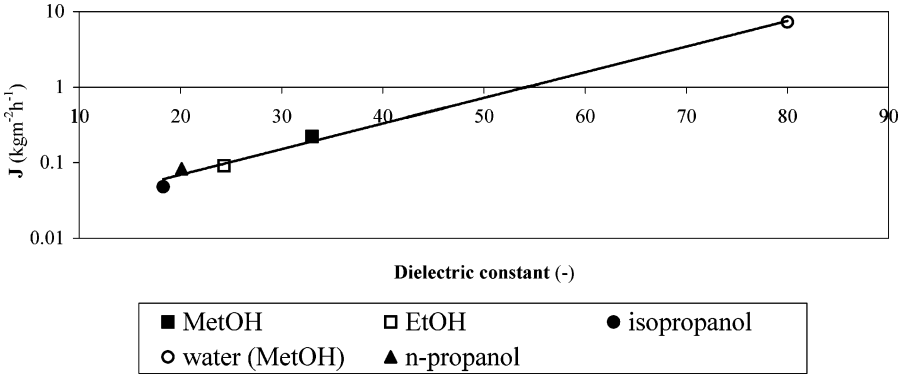

Figure 5. Flux, *J*, as a function of dielectric constant (all values taken at 50 °C).

TABLE 5: log *P* and Average Contact Angles with Their Standard Deviations

		contact angle	
	log *P*[35]	glass support	ceramic support
water	−1.38	51 ± 12	52 ± 10
MetOH	−0.63	25 ± 5	24 ± 1
EtOH	−0.14	27 ± 6	24.4 ± 0.9
2-propanol	0.28	27 ± 3	21.8 ± 0.5
n-propanol	0.35	29 ± 6	26 ± 4

component and the flux on the semilogarithmic graph in Figure 5. The major effect of polarity on flux underlines the importance of the sorption process in the pervaporative mass transport. Flux also increases with increasing dipole moment (Table 4). Water has the highest dipole moment (1.85 D). 2-Propanol has the lowest dipole moment (1.58 D). Ethanol and *n*-propanol, which have similar dipole moments (1.69 and 1.68 D, respectively), also have similar fluxes.

The final sets of parameters that can be catalogued as polarity/solubility parameters include the hydrophilicity/hydrophobicity (log *P*) of the pure component and the contact angle (combined pure component−membrane parameter). Table 5 gives an overview of their values for all components. The membrane surface tension, divided into a polar and a disperse contribution, is listed in Table 6.

Table 5 and Figure 1 show that the order of the fluxes of the various components is similar to their order of hydrophilicity. In general, a more negative log *P*, indicative of the more hydrophilic liquid, should correspond to a higher flux. However, the log *P* values for *n*-propanol and 2-propanol are in the wrong order. Other parameters, such as the aforementioned dielectric constant or Hansen parameter, are therefore more suitable to describe the flux difference between them.

TABLE 6: Average Membrane Surface Tension[a]

	glass support	ceramic support
γ^d	27	33
γ^p	20	22
γ	47 ± 7	55 ± 5

[a] γ^d, disperse component; γ^p, polar component; γ, total surface tension with standard deviation.

Contact angle measurements, using the sessile drop approach,[38] were performed on six flat, circular silica coated glass (three) and ceramic (three) plates that were heated for 5 h at 100 °C. As contact angles are low (Table 5) and (total) surface tension is high (Table 6), it is clear that the microporous silica membrane is a very hydrophilic material. The hydrophilicity of the membrane surface is a dominant parameter that influences the pure water flux through a membrane.

Water exhibits the largest contact angle. For the alcohols, no definite conclusions can be drawn with respect to the contact angles and their relation to flux, because of the large standard deviations. In part, they are the result of the support manufacturing process; while the plate is flat in the center, there is a small inclination toward the edges, resulting in wider contact angle range. However, there appears to be a small difference between the measurements performed on the glass supported and silica supported membrane top layers. The same is true when comparing surface tensions. This suggests that the characteristics of the sublayer(s) influence transport through the silica membrane. Further investigation on this matter is required.

5. Conclusions

In conclusion, it can be stated that the transport mechanism follows the adsorption−diffusion model, which comprises both

configurational (micropore) diffusion and surface diffusion. The pore flow model was not appropriate to describe transport through a microporous silica membrane.

Size parameters such as molecular weight, kinetic diameter, and effective diameter are believed to have an influence on diffusion, yet there is no correlation with flux. This emphasizes the importance of the sorption step in the pervaporation process. The good correlations with polarity parameters also support this conclusion. However, it should be kept in mind that the sublayers might also have an influence on the interaction between membrane and pure component.

The various models presented here are all based on a Fickian analysis of diffusion, and it is assumed that pure components are transported as gaseous species for which the ideal gas law applies. However, Fick's law as well as the ideal gas law may not be valid for multicomponent mixtures where coupling effects can occur. Pervaporation results of mixtures of the studied components will be evaluated thoroughly in a future paper and related to the results of the pure components.

Acknowledgment. The Research Council of the K.U. Leuven is gratefully acknowledged for financial support (OT/2002/33). Pervatech is thanked for kindly supplying membrane samples.

Glossary

A	constant in eq 6
C	concentration (mol m^{-3})
d	molecular diameter (m)
D	diffusion coefficient (m^2 h^{-1})
E_D	activation energy for diffusion (J mol^{-1})
E_F	activation energy for permeability (J mol^{-1})
E_J	activation energy for flux (J mol^{-1})
F	permeability coefficient (mol m^{-2} h^{-1} bar^{-1} or kg m^{-2} h^{-1} bar^{-1})
r_p	pore radius (m)
J	flux (mol m^{-2} h^{-1} or kg m^{-2} h^{-1})
K	Kozeny−Carman constant (-)
Kn	Knudsen number (-)
L	membrane thickness (m)
M	molecular weight (kg mol^{-1})
P	vapor pressure (bar)
P	octanol−water partition coefficient (-)
P^{vap}	vapor pressure (bar)
P_m	mean pressure over the membrane (bar)
R	gas constant (8.3143 J mol^{-1} K^{-1})
S	adsorption coefficient (mol m^{-3} bar^{-1})
S	internal surface area (m^2 m^{-3})
t	temperature (°C)
T	temperature (K)
x	feed molar fraction (-)
y	permeate molar fraction (-)

Greek Symbols

γ	activity coefficient (-)
γ	surface tension (N m^{-1})
ΔH_S	heat of adsorption (J mol^{-1})
ΔH^{vap}	heat of vaporization (J mol^{-1})
ΔP	transmembrane partial pressure difference (bar)
ϵ	porosity (-)
η	viscosity (Pa·s)
τ	tortuosity (-)

Subscripts

0	reference temperature
ads−diff	referring to adsorption−diffusion
i	component i
feed	feed
perm	permeate
mol-siev	referring to molecular sieving
surf-diff	referring to surface diffusion

Superscripts

d	disperse
mol-siev	referring to molecular sieving
p	polar
surf-diff	referring to surface diffusion

References and Notes

(1) Mulder, M. H. V. *Basic principles of membrane technology*; Kluwer: Dordrecht, The Netherlands, 1996.
(2) de Bruijn, F. T.; Sun, L.; Olujić, Ž; Jansens, P. J.; Kapteijn, F. *J. Membr. Sci*. **2003**, *223*, 141−156.
(3) Tsuru, T.; Sudou, T.; Kawahara, S.; Yoshioka, T.; Asaeda, M. *J. Colloid Interface Sci*. **2000**, *228*, 292−296.
(4) Verkerk, A. W.; Van Male, P.; Vorstman, M. A. G.; Keurentjes, J. T. F. *J. Membr. Sci*. **2001**, *193*, 227−238.
(5) van Veen, H. M.; van Delft, Y. C.; Engelen, C. W. R.; Pex, P. P. A. C. *Sep. Purif. Technol*. **2001**, *22*−*23*, 361−366.
(6) Burggraaf, A. J.; Cot, L. *Fundamentals of Inorganic Membrane Science and Technology*; Membrane science and technology series 4; Elsevier: Amsterdam, 1996.
(7) Hinchliffe, A. B.; Porter, K. E. *IChemE* **2000**, *78*(A), 255−268.
(8) de Vos, R. M.; Verweij, H. *J. Membr. Sci*. **1998**, *143*, 37−51.
(9) Sekuliæ, J.; Luiten, M. W. J.; ten Elshof, J. E.; Benes, N. E.; Keizer, K.*Desalination* **2002**, *148* (1−3), 19−23.
(10) Shieh, J.-J.; Huang, R. Y. M. *Sep. Sci. Technol.* **1998**, *33* (6), 767−785.
(11) Shieh, J.-J.; Huang, R. Y. M. *Sep. Sci. Technol*. **1998**, *33* (7), 933−957.
(12) Feng, X.; Huang, R. Y. M. *Ind. Eng. Chem. Res.* **1997**, *36*, 1048−1066.
(13) Lipnizki, F.; Trägårdh, G. *Sep. Purif. Methods* **2001**, *30* (1), 49−125.
(14) Smart, J.; Schucker, R. C.; Lloyd, D. R. *J. Membr. Sci.* **1998**, 143, 137−157.
(15) Bird, R. B.; Stewart, W. E.; Lightfoot, E. N. *Transport Phenomena*, 2nd ed.; Wiley: New York, 2002.
(16) Satterfield, C. N. *Mass transfer in heterogeneous catalysis*; M.I.T. Press: Cambridge, MA, 1970.
(17) Gilron, J.; Soffer, A. *J. Membr. Sci.* **2002**, *209*, 339−352.
(18) Sommer, S.; Melin, T.; Falconer, J. L.; Noble, R. D. *J. Membr. Sci.* **2003**, *224*, 51−67.
(19) Burggraaf, A. J. *J. Membr. Sci.* **1999**, *155*, 45−65.
(20) Wood, J.; Gladden, L. F.; Keil, F. J. *Chem. Eng. Sci.* **2002**, *57*, 3047−3059.
(21) de Lange, R. S. A.; Hekkink, J. H. A.; Keizer, K.; Burggraaf, A. J. *Microporous Mater*. **1995**, *4*, 169−186.
(22) Akin, F. T.; Lin, Y. S. Nanoporous inorganic membranes for high selectivity hydrogen separations. In *Inorganic Membranes*, Proceedings of the eighth international conference on inorganic membranes, Cincinnati, OH, July 18−22, 2004; Mansur, Y. K., Bischoff, B. L., Adcock, K. D., Powell, L. E., Judkins, R. R., Eds.; Adams Press: Chicago, 2004; pp 167−170.
(23) ten Elshof, J. E.; Abadal, C. R.; Sekulić, J.; Chowdhury, S. R.; Blank, D. H. A. *Microporous Mesoporous Mater.* **2003**, *65*, 197−208.
(24) Feng, X.; Huang, R. Y. M. *J. Membr. Sci*. **1996**, *118*, 127−131.
(25) Casado, C.; Urtiaga, A.; Gorri, D.; Ortiz, I. *Sep. Purif. Technol.* **2004**, *42* (1), 39−45.
(26) Van Baelen, D.; Reyniers, A.; Van der Bruggen, B.; Vandecasteele, C.; Degrève, J. *Sep. Sci. Technol.* **2004**, *39* (3), 563−580.
(27) Perry, R. H.; Green, D. *Perry's Chemical Engineers' Handbook*, 6th ed.; McGraw-Hill: New York, 1984.
(28) Ibert, M. *Industrial solvents handbook*, 2nd ed.; Noyes Data Corp.: Park Ridge, NJ, 1977.
(29) CRC. *Handbook of chemistry and physics*, 51st ed.; The Chemical Rubber Co.: Cleveland, OH, 1970.
(30) Bowen, T. C.; Li, S.; Noble, R. D.; Falconer, J. L. *J. Membr. Sci.* **2003**, *225*, 165−176.
(31) Hansen, C. M.; Smith, A. L. *Carbon* **2004**, *42*, 1591−1597.

(32) Yanke, L.; Shufen, Z.; Jinzong, Y.; Qinghui, W. *Colloids Surf., A* **2004**, *248*, 127−133.

(33) Hansen, C. M. *Prog. Org. Coat.* **2004**, *51*, 55−66.

(34) Shah, D.; Kissick, K.; Ghorpade, A.; Hannah, R.; Bhattacharyya, D. *J. Membr. Sci.* **2000**, *179* (1−2), 185−205.

(35) For an online log *P* calculation, see: http://www.syrres.com/esc/est_kowdemo.htm (l999−2004, Syracuse Research Corporation).

(36) Machado, D. R.; Hasson, D.; Semiat, R. *J. Membr. Sci.* **1999**, *163*, 93−102.

(37) Van der Bruggen, B. Removal of organic components from aqueous solution by nanofiltration. Doctoral Thesis, K.U. Leuven, 2000.

(38) Geens, J.; Van der Bruggen, B.; Vandecasteele, C. *Chem. Eng. Sci.* **2004**, *59* (5), 1161−1164.

(39) Olsson, J.; Trägårdh, G. *Sep. Sci. Technol.* **1999**, *34* (8), 1643−1659.

(40) Wang, K.; Qiao, S.; Hu, X. *Sep. Purif. Technol.* **2004**, *34*, 165−176.